Rapid Structured Volume Grid Smoothing and Adaption Technique

Stephen J. Alter*

NASA Langley Research Center Hampton, Virginia 23681-2199

A rapid, structured volume grid smoothing and adaption technique, based on signal processing methods, was developed and applied to the Shuttle Orbiter at hypervelocity flight conditions in support of the Columbia Accident Investigation. Because of the fast pace of the investigation, computational aerothermodynamicists, applying hypersonic viscous flow solving computational fluid dynamic (CFD) codes, refined and enhanced a grid for an undamaged baseline vehicle to assess a variety of damage scenarios. Of the many methods available to modify a structured grid, most are time-consuming and require significant user interaction. By casting the grid data into different coordinate systems, specifically two computational coordinates with arclength as the third coordinate, signal processing methods are used for filtering the data [Taubin, CG v/29 1995]. Using a reverse transformation, the processed data are used to smooth the Cartesian coordinates of the structured grids. By coupling the signal processing method with existing grid operations within the Volume Grid Manipulator tool, problems related to grid smoothing are solved efficiently and with minimal user interaction. Examples of these smoothing operations are illustrated for reductions in grid stretching and volume grid adaptation. In each of these examples, other techniques existed at the time of the *Columbia* accident, but the incorporation of signal processing techniques reduced the time to perform the corrections by nearly 60%. This reduction in time to perform the corrections therefore enabled the assessment of approximately

*Senior Aerospace Engineer, Senior Member AIAA

twice the number of damage scenarios than previously possible during the allocated investigation time.

Nomenclature

ΔS	Distance between two points
$\nabla^2 S$	Cell size stretching measure
ω	Relaxation factor
ξ,I	Streamwise computational direction and index measured from nose to tail of body
η,J	Circumferential computational direction and index from top to bottom of body
ζ,K	Body Normal computational direction and index from the body to the outer boundary

I. Introduction

On Saturday February 1, 2003, space shuttle orbiter *Columbia*, performing the Space Transportation System mission 107 (STS-107), disintegrated during Earth re-entry. In response, the *Columbia* Accident Investigation (CAI) team was formed by NASA. The Aerothermodynamic CAI (ACAI) team investigated the role of hypersonic surface heat transfer on the demise of the shuttle orbiter. The ACAI incorporated both experimental and computational methods, but this paper applies only to the computational aspects.

A single baseline structured volume grid was generated for the ACAI computational fluid dynamics (CFD) analyses,[1] and used to compute 9 sets of flow field conditions along the STS-107 trajectory. Each trajectory point was chosen based on aerodynamic requirements for a range of Mach numbers from 25 to 18. After the undamaged baseline grid was generated efficient modifications of the grids resulting from CFD solution-adapted procedures were sought for assessing orbiter damage scenarios. A traditional approach to obtain modified structured grids is regeneration, but due to the time constraints, manipulation methods of existing grid data were considered for techniques to reduce the time to develop damage scenario grids. Compounding the issue of time are the difficulties resulting from flow-field structure, vehicle shape, and differing topologies between the baseline and damage scenario surface and volume grids. By significantly reducing the time required to develop a specific structured volume grid for a damage scenario, enabled the ACAI team to provide more information to the investigation. Thus, any process that could reduce the time to obtain a

damage scenario volume grid was warranted.

Most of the grid manipulations needed to develop quality structured grids for CFD include those for grid adaptation to enable efficient use of available grid points while enhancing flow-field gradient accuracy, grid smoothing to reduce flow field gradient dissipation, and grid stretching to reduce the dispersion errors in a computation. At the time of the accident, existing grid manipulation software was limited to GridGen,[2] 3DGRAPE/AL,[3] and the Volume Grid Manipulator[4] (VGM). GridGen offers the solution of nonlinear nonhomogeneous elliptic partial differential equations (PDEs) that smooth grids, while the 3DGRAPE/AL offers a more efficient solution of the 3D PDEs. The use of PDE solvers is time-consuming because they are executed to obtain converged solutions to the PDEs, which are posed for the full set of coordinates in the volume grid. Conversely, the VGM code has algebraic smoothing methods (Ref. 4 pp61–75, 78–82) and a grid manipulation language, which are by far the fastest among smoothers. As the forensic recovery efforts progressed for the CAI, new damage scenarios emerged, producing a time criticality for developing new grids for evolving damage scenarios that could have caused the *Columbia* accident. Because algebraic manipulation methods are faster than the solution of partial differential equations used by GridGen and 3DGRAPE/AL, the reliance on the VGM software was crucial towards providing rapid changes to existing grid data.

A literature search into other disciplines inwhich mathematics is used to alter Cartesian coordinate data revealed one candidate for smoothing grids—signal processing.[5,6] Signal processing has been applied to curve and unstructured surface grid modification as a method of smoothing or reducing "noise" in the Cartesian coordinates. The "noise" is typically manifested as sharp changes in grid line character between points, as illustrated in figure 1. This method has not found application to structured volume grids and only limited application to hexahedral mesh generation[7] with wider use in the unstructured grid smoothing[8–10] community.

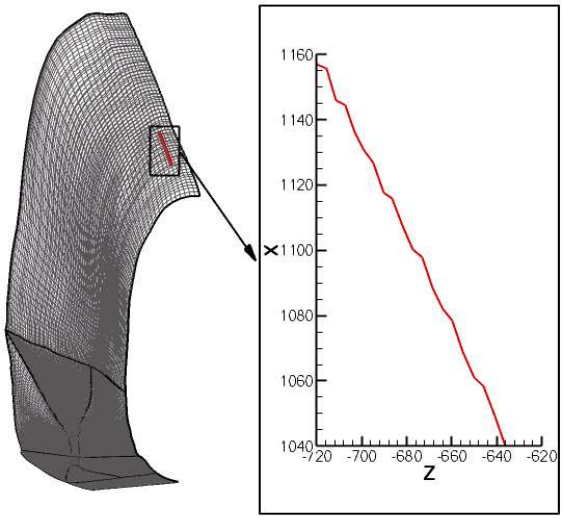

Figure 1. Structured grid identifying wave pattern for signal processing.

This paper presents the implementation and

use of signal processing technique as a structured surface and volume grid manipulation method. The use of signal processing, as confined to algebraic operators, has the ability to solve a variety of problems encountered during the generation and modification of structured grids. The manipulation method consists of a forward and backward Laplacian operator that not only smoothes grid data but also maintains the shape of the grid. Although an elliptic PDE is being used, only one variable is manipulated in the signal processing approach, the PDE is linear and it is not solved. Rather, the transient solution of the PDE is acceptable because it is the smoothing attribute of the PDE that is sought, not the final solution to the PDE. When applying the signal processing to a single variable such as arclength distance functions based on a grid in a single computational direction, the effect is grid smoothing. By switching the arclength distance function to a normalized arclength distance, the signal processing approach operates on the stretching of a grid. The signal processing methodology was successfully applied to structured grids used by the ACAI. It enabled rapid grid manipulations to smooth grids and reduce grid stretching caused by grid adaptation. In comparison to traditional methods, the signal processing approach will be shown to be significantly faster. Examples using the signal processing method will be shown for smoothing surface and volume grids, including those adapted to provide the most efficient use of available points for shock capturing CFD software.

II. Grid Generation Issues

Several grid generation issues became apparent to the ACAI through the course of attempting to develop volume grids efficiently and rapidly. They include grid adaptation which could be used to leverage existing solution-adapted grids from CFD to adapt damage scenario volume grids for outer boundary shock capturing, grid smoothing to ensure the development of quality grids used for CFD simulations, and grid stretching reduction to enable enhanced convergence of CFD flow solvers. Grid adaptation, reduction in rapid grid oscillations, and stretching reduction towards developing quality grids require grid smoothing. These grid manipulation issues are explained in more detail subsequently, with an emphasis on the issues posed to traditional solution methods.

A. Grid Adaptation

To assess the impact of leading-edge reinforced carbon-carbon (RCC) damage scenarios[11] to the aerothermodynamic environment on the shuttle orbiter, different structured grid topologies were used other than the original baseline grid,[1] as shown in figure 2.

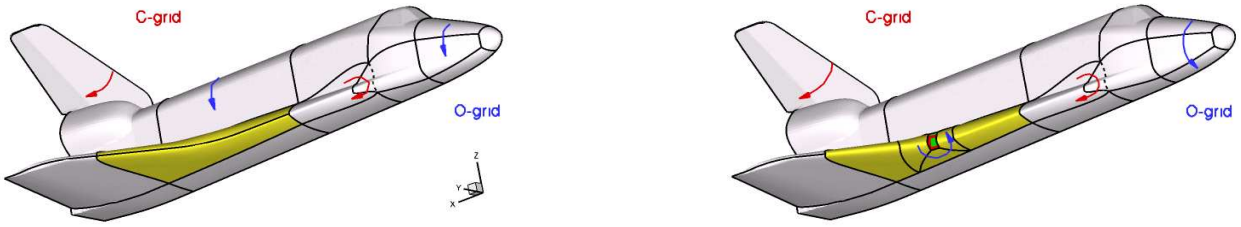

(a) Baseline.

(b) Missing RCC panel 6.

Figure 2. Structured grid topologies used for the CAI.

The region colored with a yellow shading in the mid-body region was the modified region for the damage scenarios. C- and O-grid topologies were used to decouple grid point density requirements from the remainder of the vehicle, resulting in a focusing of available grid points on the damage sites. For damage scenario CFD simulations, only the yellow portion of the flow domain was computed by using the forebody as an inflow condition and the aft body as an outflow condition to reduce the region to be computed. In all the volume grids generated, the surface grid is traversed by computational coordinates specified as I- and J-directions, and the K-direction of each grid extended from the wall to the outer boundary. This construction method used to enable the use of rapid solution-adaptive procedures.[12,13]

To reduce the time needed to generate a grid to assess the damage scenarios, the damage scenario grid was generated such that all flow conditions to be evaluated could be accommodated within the volume grid. Adapting the initial volume grid and interpolating a solution onto it from a previous common baseline grid solution provides a more accurate starting condition for the computation than restarting a solution from a free-stream initialized condition—a typical approach for CFD flow simulation tools.

Constructing a volume grid with a common computational direction between multiple volume grids but differing topologies also enabled solution and grid metric data from one grid to be transferred to the next. A traditional technique that could be used to adapt the damage scenario grid based on the baseline is to simply copy the grid point distributions in arclength along the K-direction from the baseline adapted grid to the nonadapted damage

scenario grid. Unfortunately, a one-to-one match of surface points between the baseline grid and damage scenario grids does not exist because of the different topologies, so the arclength injection is not possible in this case.

When topologies are different, traditional methods used to adapt one grid based on another involve the generation of a new volume grid based on the domain of influence from the grid with a solution. Since most grid generation methods for the size and shape of the grids used by the ACAI required approximately six weeks to build, a similar amount of time would be required to regenerate an adapted volume grid with a new topology. The six weeks include generation of the block connectors from the wall to the outer boundary, the block interfaces, and the volume grids such that similar grid metrics for orthogonality and stretching are obtained by comparison to the baseline common grid. For each flow condition, another volume grid would have to be generated. Thus, the time required to assess the STS-107 flight trajectory at 9 locations for adapted solutions on a damaged vehicle could have taken up to 54 weeks to complete for each damage scenario. Due to these limitations, the use of traditional techniques was not possible.

B. Grid Smoothing

A whole host of grid smoothers are available in the grid generation arena, ranging from rapid techniques using algebraic algorithms, which have very little control, to slower methods that have the control using the solution of nonlinear nonhomogeneous elliptic partial differential equations. An algebraic method such as trans-finite interpolation[14,15] (TFI) is used to generate an initial surface or volume grid. It can subsequently be used for smoothing or with other algebraic methods such as parametric remapping (PRM; Ref. 4 pp61–75) or Hermite vector interpolation (HVI; Ref. 4 pp78–82). However, algebraic algorithms have very little control of grid skewness and stretching, tend to produce lower quality structured grids, and do not offer shape preservation with the smoothing. The solution of elliptic PDEs using software such as GridGen or 3DGRAPE/AL is more time-consuming than algebraic methods because the equations have to be solved iteratively, and the source terms are constantly updated to obtain the required control of the grid quality. The existing grid smoothing methods are not directly applicable to the smoothing of grids that have the characteristics shown in figure 1. Rather, traditional smoothers are designed to change the entire grid or regenerate it to correct such issues.

C. Grid Stretching Reduction

As noted in the initialization procedures for structured grids using TFI, the methods are fast but tend to produce lower quality grid, manifested through skewness and grid stretching. The stretching is defined as the rate of change of distance between two adjacent cells in a computational direction. It is usually determined by dividing the largest to smallest length cells such that uniform spacing has a stretching value of unity and stretching for cells of different sizes have values greater than unity. Stretching can also be manifested through rapid changes in grid cells produced by grid adaptation procedures and round-off errors in tightly spaced grids.

Traditional methods to alleviate stretching include the solution of elliptic PDEs to smooth the grid, redistributing the grid with a similar distribution function to what was used for the construction of the grid line with significant stretching, or by using a method such as PRM to reparameterize the arclength or normalized arclength distribution functions between known reasonable reduced stretched grid lines. However, dealing with round-off errors is extremely difficult without considering changes in binary precision for the data or regenerating the grid. In all cases, significant modification of the grid is performed to reduce an otherwise subtle problem.

III. Grid Manipulation with Signal Processing

Reduction in the time required to perform grid adaptation from a baseline grid to a damage scenario grid for a specific flow-field condition remains solvable by using the K-direction mapping that is similar between the two different grids. The nonadapted RCC panel 6 grid, shown in figure 3, was constructed for the yellow region of figure 2, with the forebody and aftbody regions of the baseline common grid held fixed. Generating only the midbody for the baseline grid that contains the damage region significantly reduces the construction time from six to two weeks.[1] The original non-adapted baseline grid is used for the construction of the damage scenario grids because the single grid could be adapted to each used for multiple trajectory points, circumventing the necessity to build a specific volume grid for each Mach number and angle of attack. The leeside and windside blocks are included because the grid dimensions in the streamwise direction were increased to provide adequate resolution of the damage region. Although

there is a time savings in limiting the region to be generated, as will be show, an additional reduction in time is obtained through the application of alternative construction techniques.

As noted in the previous section, the underlying issue encountered during the generation and adaptation of the volume grids is smoothing. Two new techniques were developed to adapt and smooth volume grids that use consistent K-direction grid line topology, grid line character, and surface definition. The first technique performs the adaption, producing a grid that typically suffers from grid line roughness, while the second technique smoothes the grid lines to obtain a usable adapted grid. These two new methods are detailed in the next two subsections.

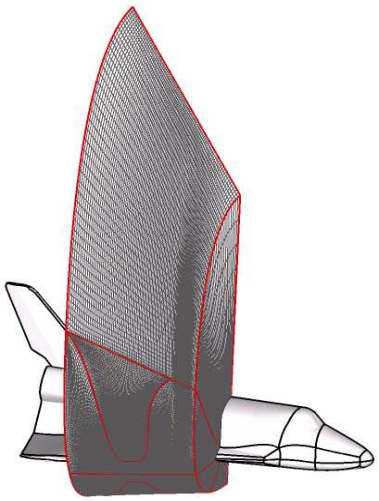

Figure 3. Original RCC panel 6 volume grid which replaces baseline midbody region.

A. Rapid Grid Adaptation

Because both the baseline common grid and the damage scenario grid were constructed on the same underlying shuttle surface geometry definition, the grids could be adapted with different topologies. The damage scenario grid is adapted by interpolating the arclength distances from the wall to each K-plane from the baseline grid to the damage scenario grid at the wall, where both volume grids share a common geometry. The tools used for this method were VGM and Tecplot.[16] By mapping the arclength distances from the wall to a specific constant K-index plane, the errors associated with summing the cell lengths in the K-direction are minimized instead of computing the lengths incrementally for each plane and adding the lengths plane by plane. Since neither VGM nor GridGen have an interpolation capability for different topologies, the Tecplot[16] software was used. As an example, figure 4 shows an adapted baseline grid and a wire frame of the block boundaries of the nonadapted damage scenario. Since the outer boundary is entirely within the limits of the RCC panel 6, no extrapolation of the damage scenario grid is needed. The adapted volume grid of the RCC panel 6 grid using the above process is shown in figure 5.

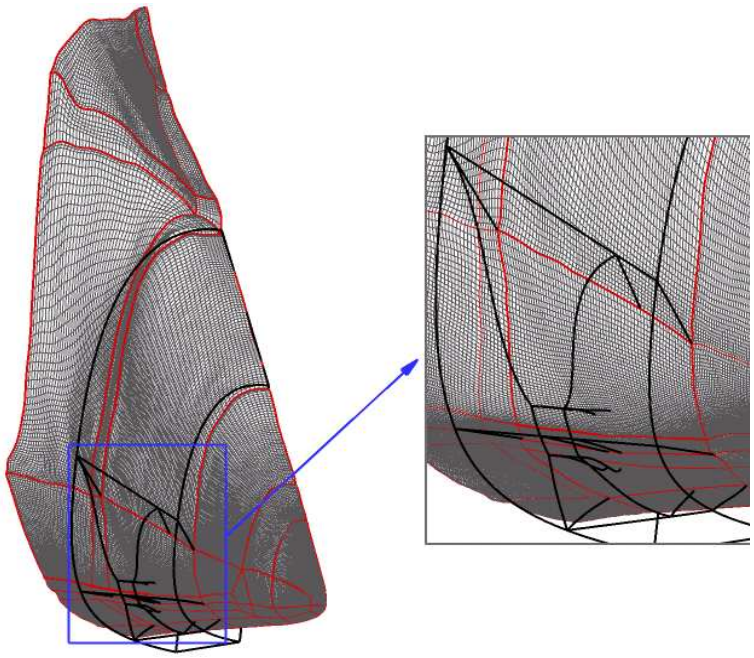

Figure 4. Baseline outer bow-shock surface with RCC-6 outline.

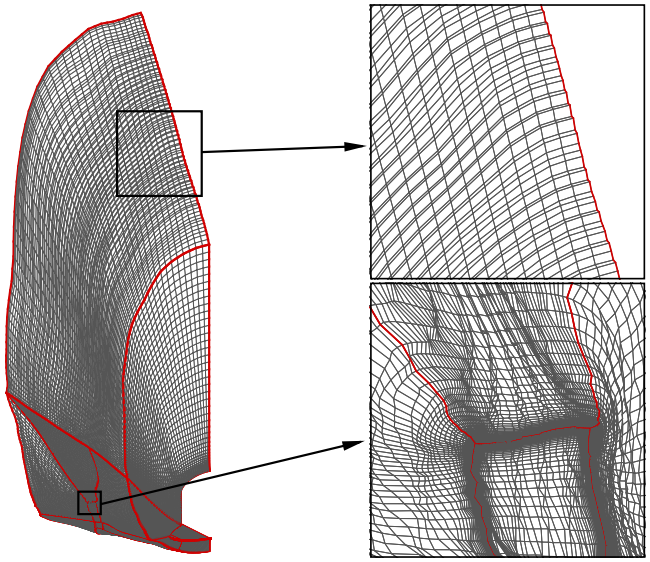

Figure 5. RCC panel 6 volume grid adaption using Tecplot interpolation of K-direction distribution functions.

By using each K-direction constant plane in the interpolation, the grid can be adapted, but dependency on grid spacing in the K-direction is lost. Without the cell spacing dependency in the K-direction, the arclength along the K-direction may not increase monotonically, which was observed in some cases. When this nonmonotonicity occurs, a simple use of three-dimensional trans-finite interpolation of the arclength distribution function in the region of the nonmonotonicity is sufficient to eliminate the condition. Hence, the adapted grid will not have crossed grid lines.

Even though no crossed grid lines occur due to the use of an arclength distance distribution function, noise is introduced into the arclength functions used for adaption during the interpolation process. Noise is manifested through the rough looking K-direction 3D surfaces, most evident at the outer boundary. The interpolation method used was first order linear interpolation in Tecplot. The linear interpolation was chosen because of speed.

B. Smoothing Adapted Grids

In order for the adaption method to work, the grid roughness has to be removed without the loss of the underlying surface; no shape change may occur. Using a solution adaptive procedure to adapt the grid was not attempted because time constraints of the fast paced CAI program would not permit researching the use. Additionally, roughness in the grid would cause adverse smearing of gradients in the flow field, which could lead to incorrect location identification of the outer bow shock. Use of a solution-adaptive procedure also requires use of a flow solver and iterations of the flow solution between applications of the method, which is time-consuming; hence, this approach was not pursued.

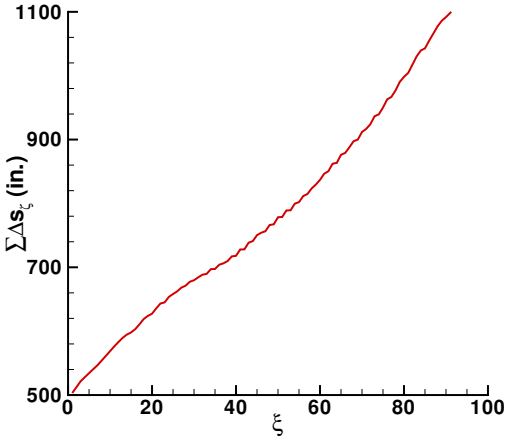

Figure 6. Arclength as a function of computational coordinate down the body, at the outer boundary.

A new method for smoothing was developed by using a signal processing approach. The analogy to signal processing, with respect to the grid, is a high frequency pattern to be filtered out of the grid without modifying the underlying lower frequency surface. The process begins by computing the K-direction arclength distribution functions for all surface

points mapped from the wall to the outer boundary. This transforms the vector field of physical coordinates into a scalar field of K-direction arclength distances. For the leeside (top) block in figure 5, an example of the arclength function in the K-direction is shown in figure 6.

Close inspection of the arclength function reveals that the distance is not smoothly changing between consecutive points. The method of Taubin[5,6] is introduced to smooth the distribution functions represented by ΔS, using a two pass approach. The first pass is nothing more than a form of a simple Laplacian operator, which, in three dimensions, takes the form of

$$\nabla^2 \Delta S = \Delta S_{\xi\xi} + \Delta S_{\eta\eta} + \Delta S_{\zeta\zeta} = 0 \tag{1}$$

where the discrete form of the derivatives are

$$\begin{aligned} \Delta S_{\xi\xi} &= \frac{\Delta S_{i-1,j,k} - 2\Delta S_{i,j,k} + \Delta S_{i+1,j,k}}{2} \\ \Delta S_{\eta\eta} &= \frac{\Delta S_{i,j-1,k} - 2\Delta S_{i,j,k} + \Delta S_{i,j+1,k}}{2} \\ \Delta S_{\zeta\zeta} &= \frac{\Delta S_{i,j,k-1} - 2\Delta S_{i,j,k} + \Delta S_{i,j,k+1}}{2} \end{aligned}$$

Expanding equation 1, and combining like terms for the center point of a three-point stencil, the equations used for the forward pass of the signal processor reduces to the unweighted average given by

$$\overline{\Delta S_{i,j,k}} = \frac{1}{6}\left[\Delta S_{i+1,j,k} + \Delta S_{i-1,j,k} + \Delta S_{i,j+1,k} + \Delta S_{i,j-1,k} + \Delta S_{i,j,k+1} + \Delta S_{i,j,k-1}\right] \tag{2}$$

On the boundaries, derivatives are only retained in the plane of the boundary. For example, on the K=1 boundary,

$$\overline{\Delta S_{i,j,1}} = \frac{1}{4}\left[\Delta S_{i+1,j,1} + \Delta S_{i-1,j,1} + \Delta S_{i,j+1,1} + \Delta S_{i,j-1,1}\right] \tag{3}$$

and along the edges of the domain, only those derivatives along the edge are retained, as given subsequently for a J=K=constant edge

$$\overline{\Delta S_{i,1,1}} = \frac{1}{2}\left[\Delta S_{i+1,1,1} + \Delta S_{i-1,1,1}\right] \tag{4}$$

and a Jacobi update point implicit relaxation step of $\omega_{forward} = 0.330$ as given by

$$\Delta S_{New} = \Delta S + 0.330 \left(\overline{\Delta S_{i,j,k}} - \Delta S \right) \tag{5}$$

where ΔS is the original arclength prior to computing the averaged arclengths from equation 2. The averaged arclengths computed in the forward pass are computed at all points within the volume domain along the surfaces and the edges. With the "new" arclengths computed, a shape recovery step is performed where the relaxation factor is negative or producing an extrapolation of the arclengths, which takes the form of

$$\Delta S_{Corrected} = \Delta S_{New} - 0.334 \left(\overline{\Delta S_{i,j,k}(New)} - \Delta S_{New} \right) \tag{6}$$

with a relaxation factor of $\omega_{backward} = -0.334$ and the Laplacian of the forward relaxed arclengths computed using equation 2 with the arclengths from equation 5. This forward and backward set of steps represents a single iteration. The number of iterations necessary may vary, so conditions on the amount of movement can be used to determine if further iterations are necessary.

The signal processing method of Taubin uses two relaxation factors, one to smooth and one to recover the shape. The shape recovery relaxation factor is always slightly larger than the smoothing relaxation factor, thus making this a low-pass filter. The values used in the present work were taken from Taubin's work as suggested values and proved to be sufficient for the smoothing of the arclength distribution functions. Although no rigorous study of relaxation was performed, the scheme remained stable and retained the smoothing properties when the order of the forward and backward steps was switched.

Another technique used to increase the speed of using the signal processing approach was the application of the method on a single block without communication among other matching blocks. Hence, each block could be solved on a separate computer central processing unit (CPU), thereby increasing the speed through a quasi-parallel processing scheme.

Using this process to smooth the arclength functions, the resulting function from figure 6 is smoothed to produce the function illustrated in figure 7. The overall shape of the distribution function is not altered, but the variations in the function are eliminated after 30 iterations. Subsequently, using these smooth arclength distribution functions to redistribute the volume grid in the K-direction results in the smoothing of the volume grid, as illustrated in figure 8. The use of the mapping of the coordinate vector field to the scalar quantity

maintains the smoothness of the grid, providing the distribution function is smooth. Basically, the signal processing method "jiggles" the grid analogous to vibrating a plate of sand with many peaks. The underlying surface is not altered, but the peaks and valleys of the grid are removed.

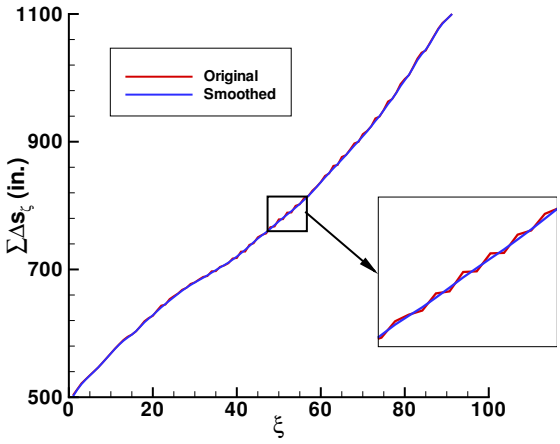

Figure 7. Smoothed arclength function, at the outer boundary.

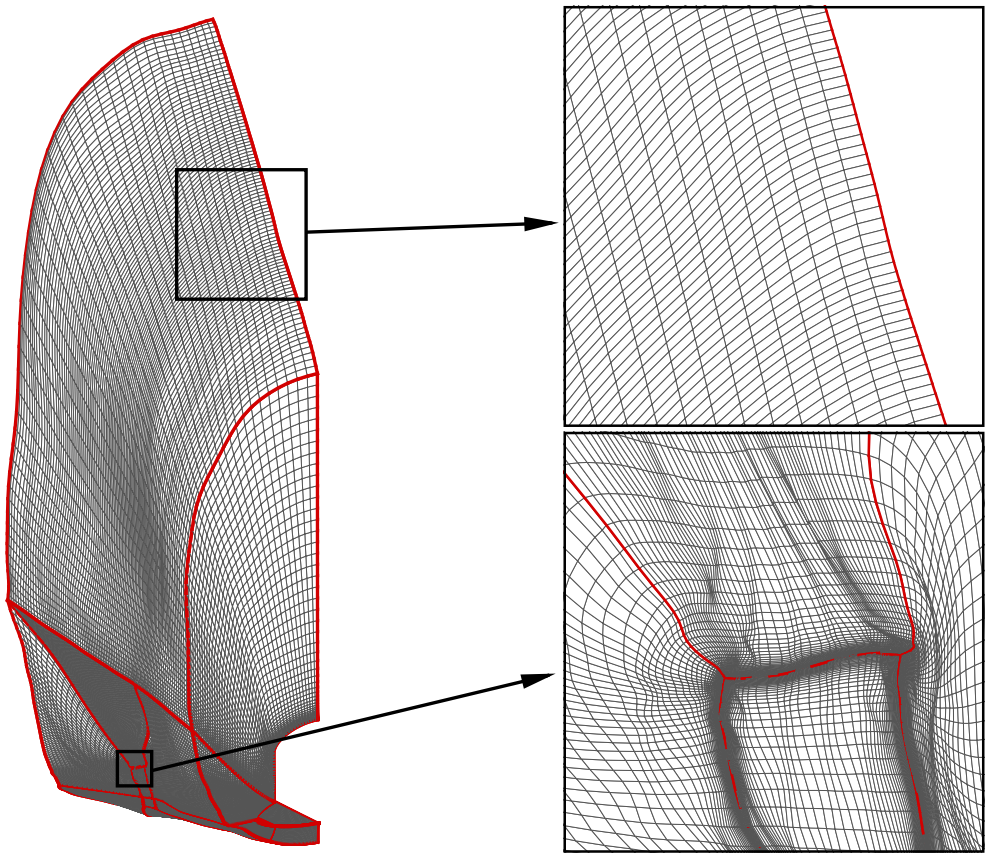

Figure 8. Adapted grid smoothed with signal processing method.

Although the volume grid in figure 8 is significantly smoother than the original in figure 5, more can be done to eliminate the subtle ripples in the grid, illustrated in the lower right-hand magnified region of figure 8. With the grid in full density, the low frequency errors are manifested as the ripples. By reducing the grid density with a sampling of every fourth point, the low frequency errors are redefined as high frequency errors, as shown in figure 9b.

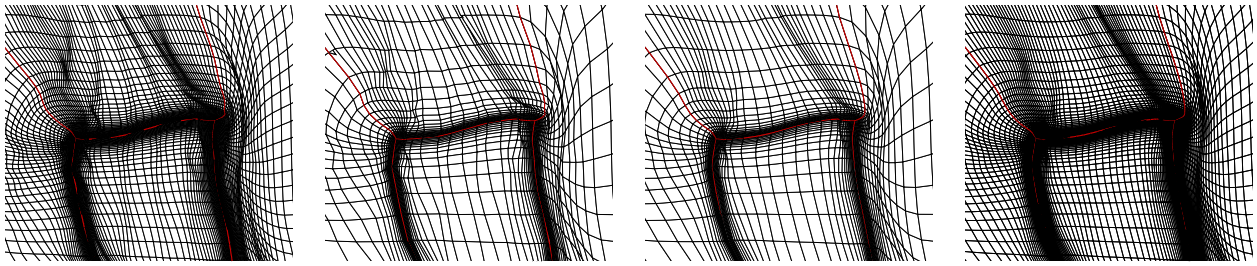

(a) Original fine grid.

(b) Original coarse grid.

(c) Smooth coarse grid.

(d) Smooth fine grid.

Figure 9. Smoothed grid using multi-grid approach for signal processing.

Using parametric remapping (PRM) on the coarsened distribution of the grid in the VGM software is not sufficient. Parametric remapping simply reconstructs the distribution functions between known points in the I- and J-directions but does not effectively handle the rapid changes in grid line character identified in figure 9b. Instead, the signal processing method used for the fine mesh is applied to the coarse mesh. The coarse mesh is constructed by using only every fourth point in each computational coordinate tangent to the wall of the vehicle, which enables the reduction of the number of iterations by a factor of two. The result is a smoothing of the coarse grid, as shown in figure 9c. The final step in the multi-grid approach is the prolongation of the K-direction arclength functions to the fine grid. These functions are determined using the PRM of VGM and are applied to the fine structured grid, resulting in a significantly smoother grid illustrated in figure 9d. The coarse grid smoothing process takes nearly one quarter the time as the fine grid smoothing. The application of the signal processing approach should be done on the fine grid first, with the multi-grid approach done second.

It took slightly more than a half hour to perform the fine grid smoothing operations, with a setup time of an additional half hour for adaptation and VGM script programming for a total of one hour to adapt and smooth the volume grid. The coarse grid smoothing operation required less than 10 minutes to complete. These times were determined from a

single user operating a single CPU SGI R12K machine. By comparison, by conducting a cursory investigation into using a solution-adaptive approach, at least an order of magnitude increase in CPU time would be required to provide the same smoothing, provided the outer boundary captured the bow shock. This measure is based on the use of several cycles of a solution-adaptive procedure for the full shuttle orbiter body decomposed to run on a couple of hundred CPUs for half an hour, with approximately 1000 iterations between grid movements. Since the signal processing approach could be used for multiple flight trajectory points because the nonadapted damage scenario grid was used for the beginning of the process, multiple combinations of flow conditions could be accommodated, one per hour.

C. Grid Stretching Reduction

Wing leading-edge damage was modeled with C-H grids, as shown in figure 10. Developing a quality grid inside a cavity with an H-grid topology, with minimal grid stretching can be a daunting task. The initial volume grid produced for the RCC cavity with the most geometric detail had maximum stretching values in excess of 3.25, as shown in figure 11. The color contours along the lines indicate the value of stretching between the cells away from the boundary identified with a thick, black line. Cells adjacent to one another in the streamwise direction of the cavity were as much as three and a quarter times larger than the next cell. This extent of stretching tends to produce convergence problems in the interior of the cavity, making an already complex physical problem more difficult to compute. Thus, the stretching had to be reduced.

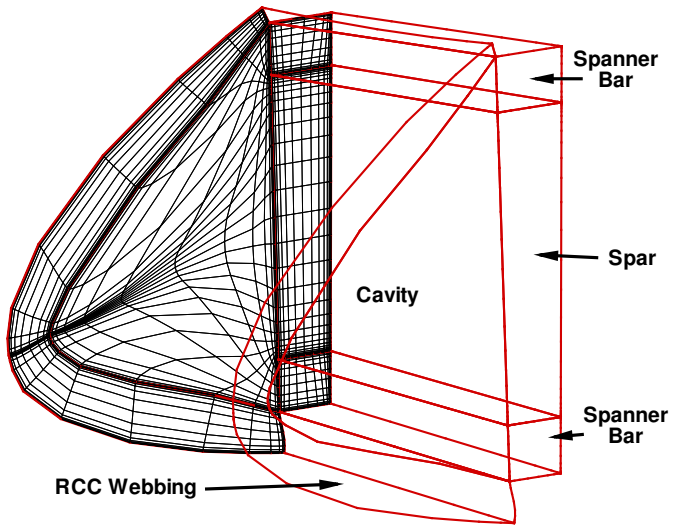

Figure 10. Detailed wing leading edge cavity geometry.

There are a number of mechanisms for reducing grid stretching. Grid points simply can be redistributed along the line they represent, or the surfaces of the point locations can be smoothed with elliptic PDEs. The problem with these approaches is that they tend to affect the entire domain and are too difficult to apply to regions that need the most stretching

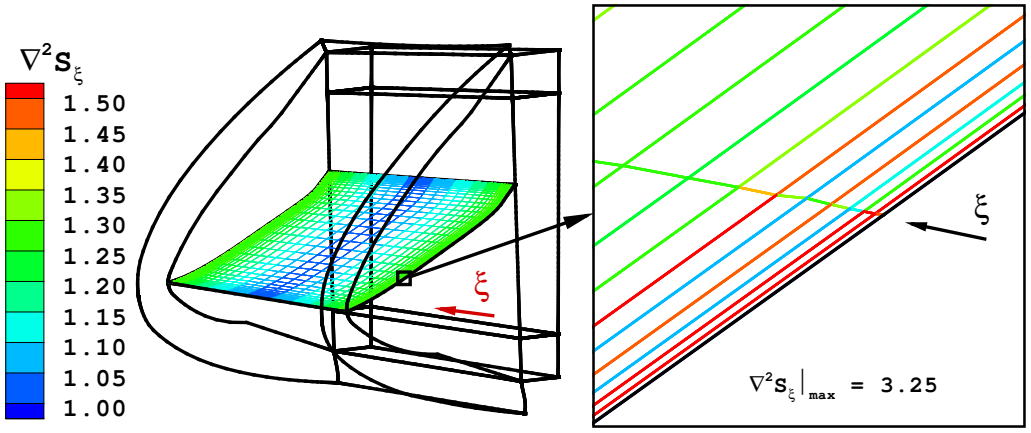

Figure 11. Stretched grid in the ξ-direction of a cavity.

reduction performed. The difficulty resides in the isolation of specific regions that have the most severe stretching. Weighting factors can be incorporated into these traditional approaches, but determining the most effective weight is not easy. Additionally, the reason for the stretching irregularities in such a small region is the result of round-off errors in the values of the coordinates. As indicated earlier, simply operating on these coordinates in a limited region tends to exacerbate the round-off issues. Hence, the signal processing approach was attempted as a mechanism of smoothing grid point distributions that define grid stretching in regions where it was warranted and not changing the grid where the stretching was acceptable for CFD simulations.

The signal to be processed is given by the stretching ratio as a function of streamwise coordinate location, as shown in figure 12a. As can be easily seen, the stretching for the majority of the grid line extending across the cavity is below the stretching factor of 1.5, a range acceptable to the ACAI. The beginning and ending regions with circled points are the locations of the most significant deviations above the 1.5 stretching factor threshold. The grid stretching values cannot be easily reconstructed in VGM; thus, the nor-

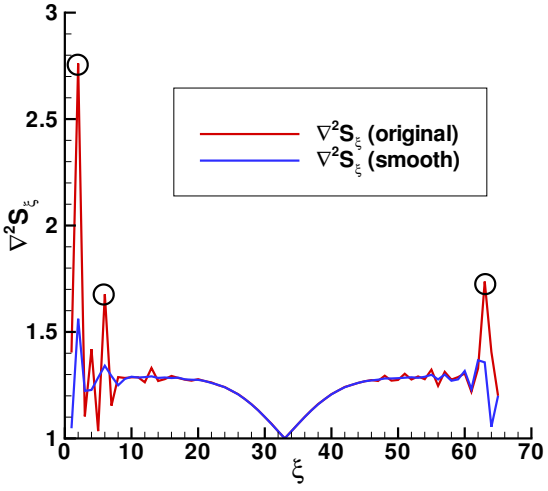

Figure 12. Grid stretching function in the streamwise direction of a cavity.

malized arclength distribution functions in the streamwise direction are smoothed. The result of smoothing the arclength distribution function has the desired effect on the grid stretching, as illustrated in figure 12.

Using the smoothed cell size distribution function to reconstruct the structured volume grid on the interior of the domain, the cavity grid is improved by reducing the grid stretching peaks at the circled points, as shown in figure 13. The peak for the smoothed signal region is now 1.55, half of the original peak, at a level that is more conducive to the accurate computation of flow-field phenomenon. This entire process required less than half an hour to prepare in the VGM software and was completed in under an hour. Furthermore, by operating on the cell size distribution functions to either increase or decrease the original values, the overall grid point locations do not move significantly, as illustrated in figure 14. At both ends of the cavity, the original grid indicated with red lines is very close to the new grid represented by blue lines. The *Imin* boundary shown in figure 14c does show more significant movement than the *Imax* shown in figure 14a; however, the movement is small.

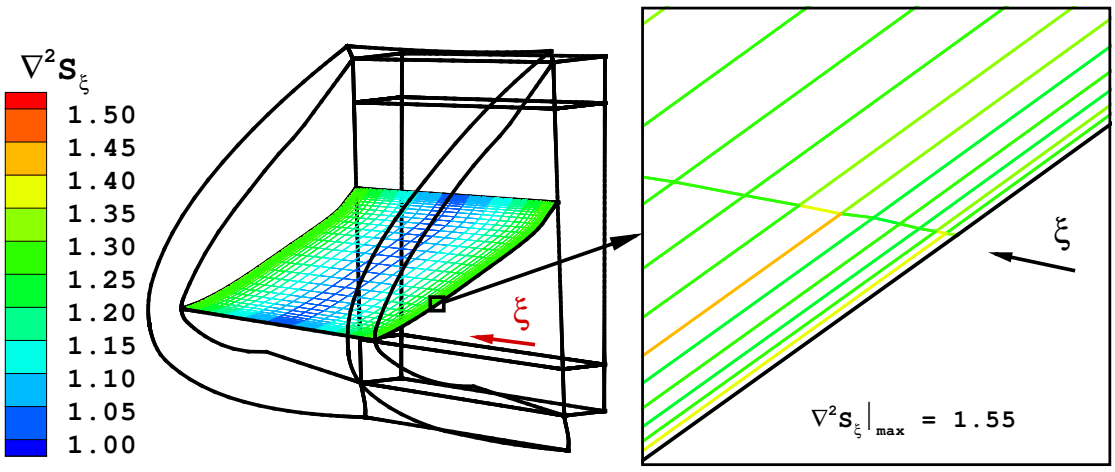

Figure 13. Stretched grid in the streamwise direction of a cavity.

IV. Summary

New structured grid smoothing and adaption techniques for volume grids are presented in this paper. A signal processing technique for grid smoothing has been available to the unstructured grid generation community for several years but finds application to volume

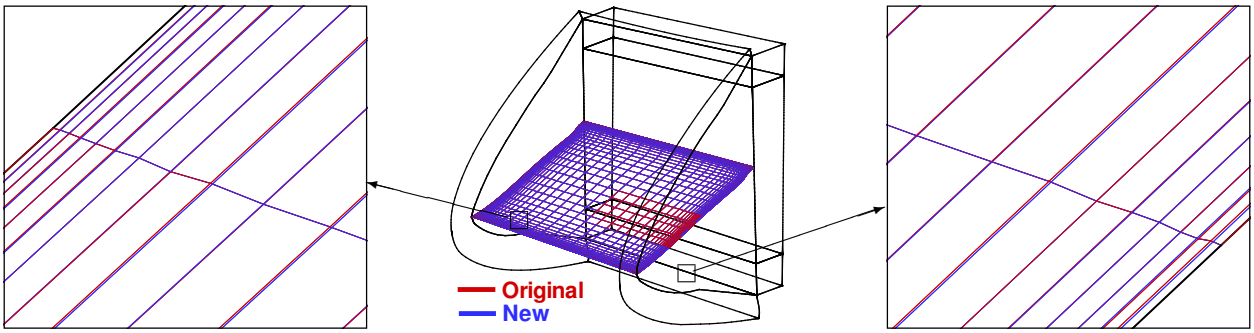

(a) *Imax* grid-stretching region.

(b) Modified grid for stretching.

(c) *Imin* grid stretching region.

Figure 14. Limits of grid-stretching reduction in the streamwise direction of a cavity.

grid manipulation. The method consists of a forward damping sweep followed by a backward shape retention sweep. The effect is a vibration of grid data to reduce the high-frequency errors or wave-like patterns in grid data.

Although application of the signal processing method is not directly used on the physical coordinates, it is used effectively on the grid-based data such as arclength functions derived from cell sizes in existing grids. Normalized cell size distribution functions are the basis for determining grid stretching and are directly related to grid skewness when compared to adjacent grid lines in a structured grid. Wave-like patterns that can be filtered with the signal processing approach include changes in normalized arclength distances from grid cell sizes that define rapid grid-stretching measures and arclengths from variational cell sizes that describe grid skewness. By smoothing the dimensional and normalized arclengths from grid distribution functions, grid skewness and grid stretching, respectively, can be reduced without significantly altering the underlying curvature of the structured grid.

There are numerous methods for smoothing structured grids, including the solution of elliptic partial differential equations and the use of algebraic methods such as trans-finite interpolation, Hermite Vector interpolation, and parametric remapping. The signal processing method contributes another tool to the existing suite of grid generation techniques. The advantages of the signal processing method is that volume grids need not be regenerated for each adapted solution if different topologies are required to model flow-field phenomenon computationally and if volume grids do not need to be elliptically smoothed for the elimination of localized grid stretching issues. Both applications are routinely required in the course of performing grid generation. The signal processing approach offers a more robust and

efficient mechanism to solve them. A significant time savings over the traditional approach of grid reconstruction, which requires two weeks, and solution-adaptive procedures, which would require days for each trajectory point, results from using signal processing for grid smoothing which amounts to a few hours. The signal processing approach used for the STS-107 investigation enabled rapid turnaround of grids used on damage scenario assessments with enhanced grid quality while reducing generation time.

References

[1]Alter, S. J., Reuther, J. J., and McDaniel, R. D., "Development of a Flexible Framework of Common Hypersonic Navier-Stokes Meshes for the Space Shuttle Orbiter," AIAA Paper 2004–2635, June 2004.

[2]J. P. Steinbrenner, Chawner, J. R., and Fouts, C. L., "The GRIDGEN 3D Multiple Block Grid Generation System," Wright Research and Development Center Report TR–90–3022, July 1990.

[3]Alter, S. J., "Efficient Development of High Fidelity Structured Volume Grids for Hypersonic Flow Simulations," AIAA Paper 2003–0952, January 2003.

[4]Alter, S. J., *The Volume Grid Manipulator (VGM): A Grid Reusability Tool*, No. 4772, NASA Contractor Report, April 1997.

[5]Taubin, G., "A Signal Processing Approach to Fair Surface Design," *Computer Graphics*, Vol. 29, 1995, pp. 351–358.

[6]Taubin, G., "Curve And Surface Smoothing Without Shrinkage," *ICCV 95*, 1995, pp. 852–857.

[7]Tchon, K. and Schneiders, R., "Octree-Based Hexahedral Mesh Generation for Viscous Flow Simulations," *5th International Meshing Roundtable*, Sandia National Laboratories, October 1996, pp. 205–216.

[8]Schkolne, S. and Schröder, P., "Surface drawing," Caltech Department of Computer Science CS–TR–99–03, 1999.

[9]Buhler, K., Felkel, P., and La Cruz, A., "Geometric Methods for Vessel Visualization and Quantification - A Survey," Tech. Rep. TR-VRVis 2003-035, 2003.

[10]Huber, D., *Automatic Three-dimensional Modeling From Reality*, Ph.D. thesis, Carnegie Mellon University - The Robotics Institute, July 2002.

[11]Pulsonetti, M. V., Thompson, R. A., and Buck, G. M., "LAURA Computations of the Space Shuttle *Columbia* STS-107 Baseline and Damaged Configurations," AIAA Paper 2004–2278, June 2004.

[12]Gnoffo, P. A., "Upwind-Biased, Point-Implicit Relaxation Strategies for Viscous Hypersonic Flows," AIAA Paper 89–1972, June 1989.

[13]Gnoffo, P. A., "An Upwind–Biased Point–Implicit Relaxation Algorithm for Viscous, Compressible Perfect–Gas Flows," NASA Technical Paper 2953, February 1990.

[14]Gordon, W. J. and Hall, C. A., "Construction of Curvilinear Coordinate Systems and Applications to Mesh Generation," *International Journal of Numerical Methods in Engineering*, Vol. 3, No. 7, July 1973, pp. 461–477.

[15]Soni, B. K., "Two– and Three–Dimensional Grid Generation for Internal Flow Applications of Computational Fluid Dynamics," AIAA Paper 85–1526, 1985.

[16]Amtec Engineering Inc., "Tecplot: version 9 User's Manual," Amtec Engineering publication V9.0/2001, August 2001.